Original Article

Assessment of elastographic Q-analysis score combined with Prostate Imaging-Reporting and Data System (PI-RADS) based on transrectal ultrasound (TRUS)/multi-parameter magnetic resonance imaging (MP-MRI) fusion-guided biopsy in differentiating benign and malignant prostate

Hongtian Tian[#], Zhimin Ding[#], Huaiyu Wu, Keen Yang, Di Song, Jinfeng Xu, Fajin Dong

Department of Ultrasound, First Affiliated Hospital of Southern University of Science and Technology, Second Clinical College of Jinan University, Shenzhen Medical Ultrasound Engineering Center, Shenzhen People's Hospital, Shenzhen, China

Contributions: (I) Conception and design: Z Ding, H Tian; (II) Administrative support: J Xu, F Dong; (III) Provision of study materials or patients: H Tian; (IV) Collection and assembly of data: H Wu, Di Song, K Yang, H Tian; (V) Data analysis and interpretation: K Yang, H Tian; (VI) Manuscript writing: All authors; (VII) Final approval of manuscript: All authors.

[#]These authors contributed equally to this work and should be considered as co-first authors.

Correspondence to: Jinfeng Xu, MD; Fajin Dong, MD. Department of Ultrasound, First Affiliated Hospital of Southern University of Science and Technology, Second Clinical College of Jinan University, Shenzhen Medical Ultrasound Engineering Center, Shenzhen People's Hospital, No. 1017 Dongmen North Road, Shenzhen 518020, China. Email: xujinfeng@yahoo.com; dongfajin@szhospital.com.

Background: Magnetic resonance imaging (MRI) has advantages in the diagnosis of prostate diseases, but there is also overdiagnosis. We compensate for this with fusion imaging and elastography. In this study, we want to evaluate Elastographic Q-analysis score (EQS) combined with Prostate Imaging Reporting and Data System (PI-RADS), based on transrectal ultrasound (TRUS)/multi-parameter magnetic resonance imaging (MP-MRI) fusion biopsy in differentiating benign and malignant prostate lesions.

Methods: A total of 296 patients with 318 prostate lesions who underwent TRUS/MP-MRI fusion biopsy between October 2017 and October 2019 were retrospectively analysed. The performance of the EQS was evaluated on the sites of the suspicious areas of MP-MRI. The cut-off value of EQS was obtained according to receiver operating characteristic (ROC) curve, which was used to upgrade and downgrade the PI-RADS scores. The area under the curve (AUC), integrated discrimination improvement, and decision curve analysis were used to assess the new PI-RADS performance.

Results: In total, 318 MP-MRI suspicious prostate lesions (94 malignant *vs.* 224 benign lesions). The EQS optimal threshold was 1.85, and the AUC was 0.816. All cases were constructed three models by using 1.85 as the cut-off value: upgrade-PI-RADS, downgrade-PI-RADS and complex-PI-RADS. The AUC of PI-RADS, upgrade-PI-RADS, downgrade-PI-RADS and complex-PI-RADS were 0.869, 0.867, 0.872 and 0.873 respectively. The diagnostic coincidence rate of PI-RADS was increased from 0.667 to 0.874 by using strain elastography, among which the diagnostic rate of prostate cancer was increased from 0.557 to 0.806, and the diagnostic rate of non-prostate cancer was increased from 0.775 to 0.967. The integrated discrimination improvement indicated that downgrade-PI-RADS had a better diagnostic capability ($P<0.05$). The net benefit of all models, which downgrade-PI-RADS can maximize the net benefit value of patients by decision curve analysis.

Conclusions: The combination of PI-RADS and EQS with TRUS/MP-MRI fusion, particularly downgrade-PI-RADS, can reduce unnecessary biopsy procedures and prevent overdiagnosis.

Keywords: Transrectal ultrasound (TRUS); elastography; Prostate Imaging-Reporting and Data System (PI-RADS); prostate cancer (PCa); image fusion biopsy

Submitted Sep 18, 2021. Accepted for publication Mar 28, 2022.
doi: 10.21037/qims-21-932
View this article at: https://dx.doi.org/10.21037/qims-21-932

Introduction

Prostate cancer (PCa) is the second most common malignant tumour among the male population worldwide (1), posing a significant threat to men's health. Multi-parameter magnetic resonance imaging (MP-MRI) is being used increasingly in the diagnosis of PCa and has emerged as a valuable imaging modality in PCa detection, staging, and active surveillance (2-4). The first version of Prostate Imaging-Reporting and Data System (PI-RADS) was published by the European Society of Urogenital Radiology in 2012, and the PI-RADS version 2.1 came into use in 2019 (5). MP-MRI is the most sensitive imaging technique in the detection of localized PCa, however, its specificity is limited. Some regions might be mistakenly considered as malignant pathological conditions (6).

Ultrasound elastography is an emerging imaging method that can show the stiffness of the tissue. PCa tissue is usually stiffer than the surrounding normal tissue (7). Some studies suggest that elastography could improve the detection of PCa better than systemic biopsies (8,9), thus reducing the number of biopsy procedures (10). Other studies have also proven that there was a significant positive correlation between the strain index and the Gleason score (11-13).

Elastographic Q-analysis score (EQS) software is a semi-quantitative analysis based on strain elastography. Conventional strain elasticity responds to the instantaneous stiffness of the tissue, while EQS reflects the stiffness change of the tissue during 2,000 ms. Comparing with the traditional strain elasticity, EQS has higher accuracy and better repeatability. Our previous research showed that the EQS could improve the accuracy of diagnosing, grading PCa (14-16).

The purpose of this study was to improve the diagnosis of PCa and reduce unnecessary biopsies by combining the PI-RADS with the EQS. We present the following article in accordance with the STARD reporting checklist (available at https://qims.amegroups.com/article/view/10.21037/qims-21-932/rc).

Methods

Patients

This study consecutively included patients who underwent prostate biopsy in the ultrasound department between October 2017 and October 2019. The study was conducted in accordance with the Declaration of Helsinki (as revised in 2013) and was approved by the Ethics Committee of Shenzhen People's Hospital. All patients provided signed informed consent. The inclusion criteria were as follows: the patients should meet clinical biopsy indications. Such as, abnormal prostate-specific antigen (PSA) levels—both PSA =4–10 ng/mL and free PSA (fPSA)/PSA <0.16, PSA >10 ng/mL—and positive digital rectal examination, and must express willingness to undergo to the procedure. All patients must have undergone MP-MRI prior to biopsy.

The exclusion criteria were as follows: being unable to tolerate or consent to MP-MRI, transrectal ultrasound (TRUS), or biopsy and having no obvious lesions on the MP-MRI image.

In total, 296 patients who underwent TRUS/MP-MRI fusion biopsy and 318 prostate lesions detected at our hospital from October 2017 to October 2019 were included.

Equipment

The magnetic resonance apparatus used was a Siemens Magnetom Skyra 3.0-T scanner (Siemens Germany) with a superconductive magnet. The ultrasonic diagnostic equipment we used was a LOGIQ E9 colour Doppler ultrasound instrument (GE Healthcare, Little Chalfont, England) with a volume navigation system and an IC5-9-D cavitary transducer. We chose a TSK 18-gauge

automatic biopsy gun (TSK Laboratory, Oisterwijk, the Netherlands) for TRUS-guided prostate biopsy. Prior to the biopsy, we also acquired a sterile condom and coupling gel.

Procedures

Before the biopsy

All patients underwent MP-MRI. Before the MRI examination, all were informed to urinate a small amount, and were scanned 1cm above the public symphysis. The scanning scope included at least the prostate and seminal vesicle. Imaging included T2-weighted imaging (T2WI) sequence (including the cross section, sagittal plane, and coronal plane), diffusion-weighted imaging (DWI) generated by single-shot spin echo planar imaging (SS-EPI) sequence, and dynamic contrast-enhanced MRI (DCE-MRI) was generated by fat-suppressed T1-weighted imaging (T1WI) sequence with 3D spoiled gradient echo, after rapid intravenous injection with gadopentetate dimeglumine (0.2 mmol/kg). Image evaluation was conducted, and the structured PI-RADS version 2 report was prepared by two experienced radiologists together (J Xu with over 25 years working experience and F Dong with 15 working experience).

During the prostate biopsy

First, the patient's Digital Imaging and Communications in Medicine data of MRI were transferred to the ultrasonic diagnostic apparatus. Image fusion consisted of plane-to-plane registration, and by point-to-point registration. All registrations were performed in the axial plane. We used muscoli puborectalis as the primary plane for image fusion. Then, based on patients' conditions, different points such as calcification, cysts and urethral orifices were selected. Subsequently, the MRI of the reference plane and selected points were matched by the overlay mode to increase observational accuracy. Secondly, TRUS was examined. At the same time, the MP-MRI and TRUS images were fused, and we applied a slight force to the lesions which were detected on MRI in order to obtain the video of strain elastography. Z Ding with over 25 years working experience performed the TRUS, and did biopsies with the guiding device. Thirdly, importing the video into the EQS software, and placing the sampling box in the suspicious area of the fusion image. Turning on smooth mode to reduce interference from uneven external forces. The software is used to analyse the average elasticity score taking 2,000 ms. Finally, targeted MP-MRI/TRUS fusion-guided prostate biopsy 2-core and systematic 12-core biopsy were performed.

Statistical analyses

All analyses were conducted in SPSS version 25.0 software (IBM Corporation, Armonk, NY, USA) and RStudio v1.3 (SAS Institute, Inc., Cary, USA). Figures were assembled with Illustrator software (Adobe Illustrator CS6, California, USA). *T*-test was used for numerical variables with normal distribution, chi-square test was used for categorical variables with normal distribution, and rank sum test was used for variables with non-normal distribution. $P<0.05$ was considered statistical significance. The thresholds were obtained by receiver operating characteristic (ROC) curve and Youden index (17). The performances of different models were assessed by s curve, integrated discrimination improvement (IDI) and decision curve analysis (DCA). Prostate volume was measured based on TRUS and calculated using multiplying 0.52 with the diameters of the prostate gland from three different axes (up-down, left-right, and front-rear).

Results

Patient characteristics and pathologic features

A total of 457 persons prostate biopsies were performed between October 2017 and October 2019. Patients who hadn't been performed prostate MRI or hadn't been performed prostate MRI in our hospital (n=98), hadn't been performed elastography (n=37), and did only systemic biopsies (n=26). In total, 296 patients were included, and 318 lesions (94 malignant, 224 benign) were detected (*Figure 1*). Twenty patients had 2 lesions, and one patient had 3 lesions. The baseline clinical character of these patients was presented in *Table 1*.

PCa diagnosis by EQS

According to the EQS score and biopsy results, an ROC curve was constructed. The Youden index was 0.609, the EQS optimal threshold was 1.85, and the area under the curve (AUC) was 0.816 [95% confidence interval (CI): 0.762–0.870] (*Figure 2*).

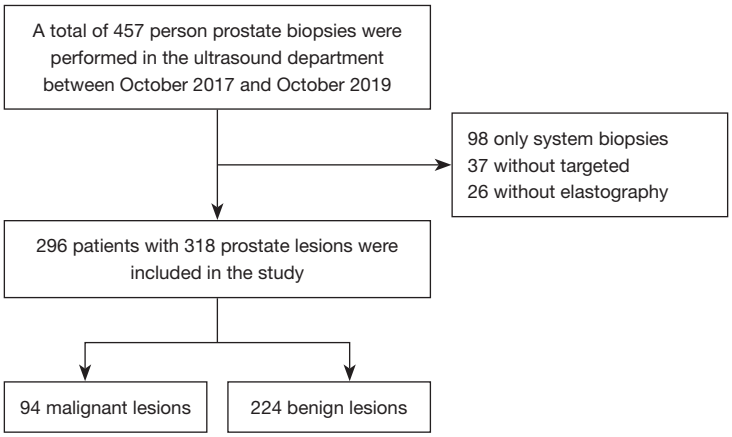

Figure 1 Flow chart.

Table 1 Baseline clinical characteristics of the final study cohort

Variables	Total (n=318)	Benign (n=224)	Malignant (n=94)	P
Age (years), mean ± SD	66.64±8.76	65.38±8.54	69.65±8.58	<0.001
fPSA (ng/mL), median (IQR)	1.45 (0.91, 2.62)	1.35 (0.88, 1.98)	2.34 (1.07, 6.36)	<0.001
PSA (ng/mL), median (IQR)	10.48 (6.75, 20.14)	9.04 (6.17, 14.01)	23.39 (9.80, 59.48)	<0.001
fPSA/PSA, median (IQR)	0.13 (0.09, 0.18)	0.15 (0.11, 0.20)	0.10 (0.07, 0.14)	<0.001
Volume (mL), median (IQR)	47.44 (37.67, 65.56)	48.59 (38.09, 64.09)	45.31 (35.61, 66.22)	0.227
PSAD, median (IQR)	0.21 (0.14, 0.44)	0.18 (0.12, 0.28)	0.48 (0.24, 1.11)	<0.001
EQS, median (IQR)	1.5 (1.1, 2.5)	1.2 (1.0, 1.7)	2.6 (2.02, 3.4)	<0.001
PI-RADS, n [%]				<0.001
2	38 [12]	37 [17]	1 [1]	
3	122 [38]	113 [50]	9 [10]	
4	105 [33]	71 [32]	34 [36]	
5	53 [17]	3 [1]	50 [53]	

EQS, elastographic Q-analysis score; PSA, prostate-specific antigen; fPSA, free PSA; PSAD, PSA density; PI-RADS, Prostate Imaging-Reporting and Data System; SD, standard deviation; IQR, interquartile range.

Combined with PI-RADS

Pathological results, PI-RADS results and EQS score of lesions were shown in *Table 2*. All cases were constructed three models by using 1.85 as the cut-off value (Table S1):

- Model upgrade-PI-RADS: when lesions' PI-RADS were 2 or 3 and whose EQS >1.85, the lesions were upgraded to PI-RADS 4. The rest lesions PI-RADS with EQS ≤1.85 did not change.
- Model downgrade-PI-RADS: when lesions' PI-RADS were 4 or 5 and whose EQS ≤1.85, the lesions were downgraded to 3. The rest lesions PI-RADS with EQS >1.85 did not change.
- Model complex-PI-RADS: when EQS >1.85, the lesions of PI-RADS 2 or 3 upgraded to 4, in the same time lesions of PI-RADS 4 or 5 downgraded to 3 when EQS ≤1.85.

According to the PI-RADS, new PI-RADS (upgrade-PI-RADS, downgrade-PI-RADS, and complex-PI-RADS) and considering the biopsy results as a golden standard, the ROC curve was reconstructed and the AUC (95% CI) were 0.869 (0.827–0.911), 0.867 (0.825–0.909), 0.872 (0.823–0.920) and 0.873 (0.828–0.918) respectively (*Figure 2*).

The optimal threshold of upgrade-PI-RADS, downgrade-PI-RADS, and complex-PI-RADS was 4 based

on the ROC curve (*Figure 2*). PI-RADS scores were divided into groups greater than or equal to 4 and less than 4, and then the pathology results were compared. The coincidence rate (CR), true-positive (TP), false-positive (FP), true-negative (TN), false-negative (FN) values, sensitivities, specificities, positive likelihood ratio (LR+), negative likelihood ratio (LR–), negative predictive value (NPV) and positive predictive value (PPV) were calculated in *Table 3*. In the same time, we also calculated the diagnostic capacity of PI-RADS and EQS in *Table 3*.

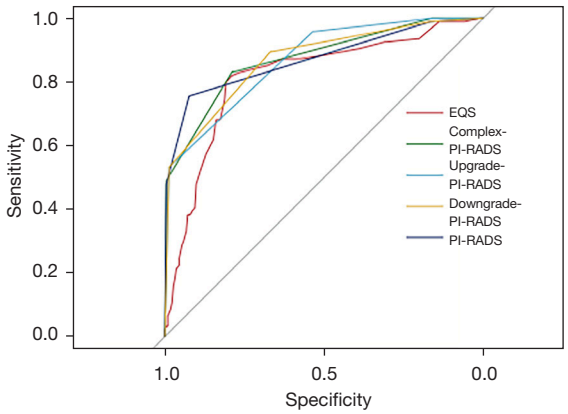

Figure 2 ROC of the EQS, PI-RADS, upgrade-PI-RADS, downgrade-PI-RADS, and complex-PI-RADS. ROC, receiver operating characteristic; EQS, elastographic Q-analysis score; PI-RADS, Prostate Imaging-Reporting and Data System.

Models performance

AUC indicated that complex-PI-RADS and downgrade-PI-RADS had basically the same diagnostic capability, while IDI indicated that downgrade-PI-RADS had a better diagnostic capability (IDI =10.3‰, P<0.05), but the performance of both of them were better than PI-RADS (complex-PI-RADS *vs.* PI-RADS: –3.0‰, downgrade-PI-RADS *vs.* PI-RADS: 13.3‰). PI-RADS performed better than upgrade-PI-RADS. See *Figure 3A* and *Table 4* for details.

Clinical use

Net benefit (NB) was plotted by DCA. We calculated the NB of all models, which downgrade-PI-RADS can maximize the NB value of patients (*Figure 3B*).

Discussion

Our study found that EQS has a good diagnostic capability,

Table 2 Pathological results, PI-RADS results and EQS score of lesions

EQS	PI-RADS and pathology (PCa)*				
	PI-RADS 2	PI-RADS 3	PI-RADS 4	PI-RADS 5	Total
>1.85	2 [1]	34 [5]	41 [25]	47 [46]	124 [77]
≤1.85	36 [0]	88 [4]	64 [9]	6 [4]	194 [17]
Total	38 [1]	122 [9]	105 [34]	53 [50]	318 [94]

*, data in parentheses are the number of PCa. PI-RADS, Prostate Imaging-Reporting and Data System; EQS, elastographic Q-analysis score; PCa, prostate cancer.

Table 3 Diagnostic capacity of PI-RADS, upgrade-PI-RADS, downgrade-PI-RADS, complex-PI-RADS and EQS

Models	CR	Sens.	Spec.	LR+	LR–	NPV	PPV	AUC
PI-RADS	0.667	0.557	0.775	2.475	0.572	0.639	0.710	0.869
EQS	0.799	0.819	0.790	3.904	0.229	0.912	0.621	0.816
Upgrade-PI-RADS	0.660	0.463	0.967	14.381	0.554	0.535	0.957	0.867
Downgrade-PI-RADS	0.874	0.806	0.900	8.068	0.215	0.924	0.755	0.872
Complex-PI-RADS	0.802	0.624	0.917	7.527	0.410	0.790	0.829	0.873

AUC, area under the curve; PI-RADS, Prostate Imaging-Reporting and Data System; EQS, elastographic Q-analysis score; CR, coincidence rate; Sens., sensitivities; Spec., specificities; LR+, positive likelihood ratio; LR–, negative likelihood ratio; NPV, negative predictive value; PPV, positive predictive value.

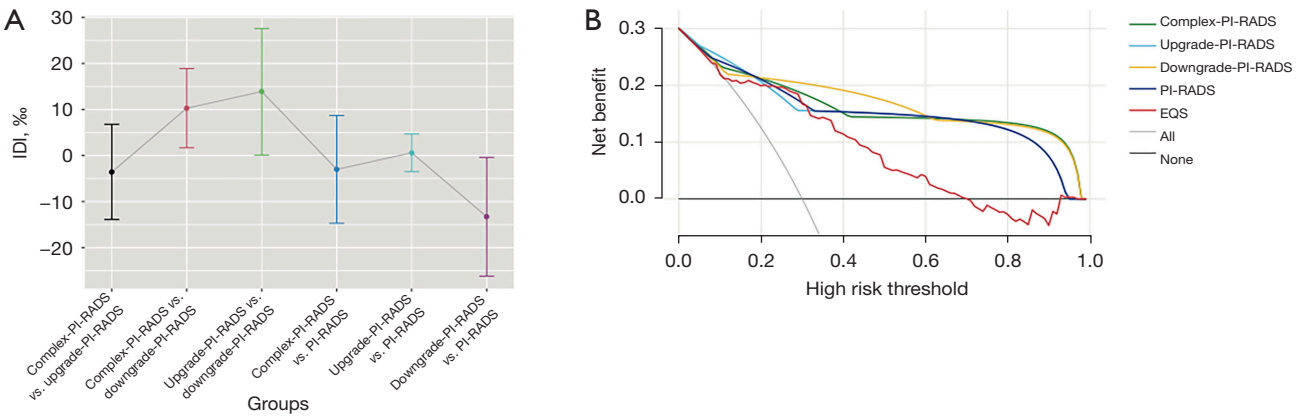

Figure 3 Risk-return comparison between different models. (A) Risk variation between two models was assessed by IDI. (B) DCA of EQS, PI-RADS, upgrade-PI-RADS, downgrade-PI-RADS, and complex-PI-RADS. IDI, integrated discrimination improvement; PI-RADS, Prostate Imaging-Reporting and Data System; EQS, elastographic Q-analysis score; DCA, decision curve analysis.

Table 4 Risk variation between two models was assessed by IDI

Comparison of models	IDI (‰)	95% CI (‰)	P
Complex-PI-RADS *vs.* upgrade-PI-RADS	−3.6	−13.9 to 6.8	0.50
Complex-PI-RADS *vs.* downgrade-PI-RADS	10.3	1.7 to 18.9	0.02
Upgrade-PI-RADS *vs.* downgrade-PI-RADS	13.9	0.1 to 27.6	0.05
Complex-PI-RADS *vs.* PI-RADS	−3.0	−14.7 to 8.7	0.62
Upgrade-PI-RADS *vs.* PI-RADS	0.6	−3.5 to 4.7	0.77
Downgrade-PI-RADS *vs.* PI-RADS	−13.3	−26.2 to −0.4	0.04

CI, confidence interval; IDI, integrated discrimination improvement; PI-RADS, Prostate Imaging-Reporting and Data System.

but the combination of PI-RADS and EQS demonstrated better diagnostic performance than PI-RADS or EQS alone. According the results of IDI, AUC and DCA, downgrade-PI-RADS had the best performance, and complex-PI-RADS is slightly inferior to downgrade-PI-RADS. The performance of upgrade-PI-RADS was not satisfactory. We find that downgrade-PI-RADS and complex-PI-RADS had better CR, and the CR of downgrade-PI-RADS is up to 0.874, which was higher than PI-RADS alone. Although the EQS had higher sensitivities, it had the lowest NB in terms of DCA. When diagnosing non-PCa, the combination of PI-RADS and EQS was also superior to PI-RADS alone (specificities: 0.967 *vs.* 0.775). The LR+ of upgrade-PI-RADS, downgrade-PI-RADS, and complex-PI-RADS are higher than PI-RADS, only upgrade-PI-RADS exceeds 10. In the same time, LR– of upgrade-PI-RADS, downgrade-PI-RADS, and complex-PI-RADS are lower than PI-RADS, but none of them is less than 0.1. Among the NPV and PPV, upgrade-PI-RADS and downgrade-PI-RADS exceed 0.9 respectively.

MP-MRI has become a major tool for the diagnosis of PCa (18,19). The generalization of the clinical application of the PI-RADS has witnessed the success of the PI-RADS itself. However, it is not flawless, and there are still some drawbacks in its clinical application, for example, benign lesions, such as prostatitis, scarring, high-grade prostatic intraepithelial neoplasia, and hyperplasia, mimic the characteristics of PCa and thus lower the specificity. Elastography can make up for certain deficiencies in diagnosing benign and malignant prostate lesions.

Elastography can guide prostate biopsy and detect more clinically significant PCa cases (20,21). The EQS based on strain elastography has some advantages. It represents the average of the stiffness fluctuation in target area during 2,000 ms, not the instant stiffness. Thereby achieving a stable elastographic result if the curve is straight and parallel

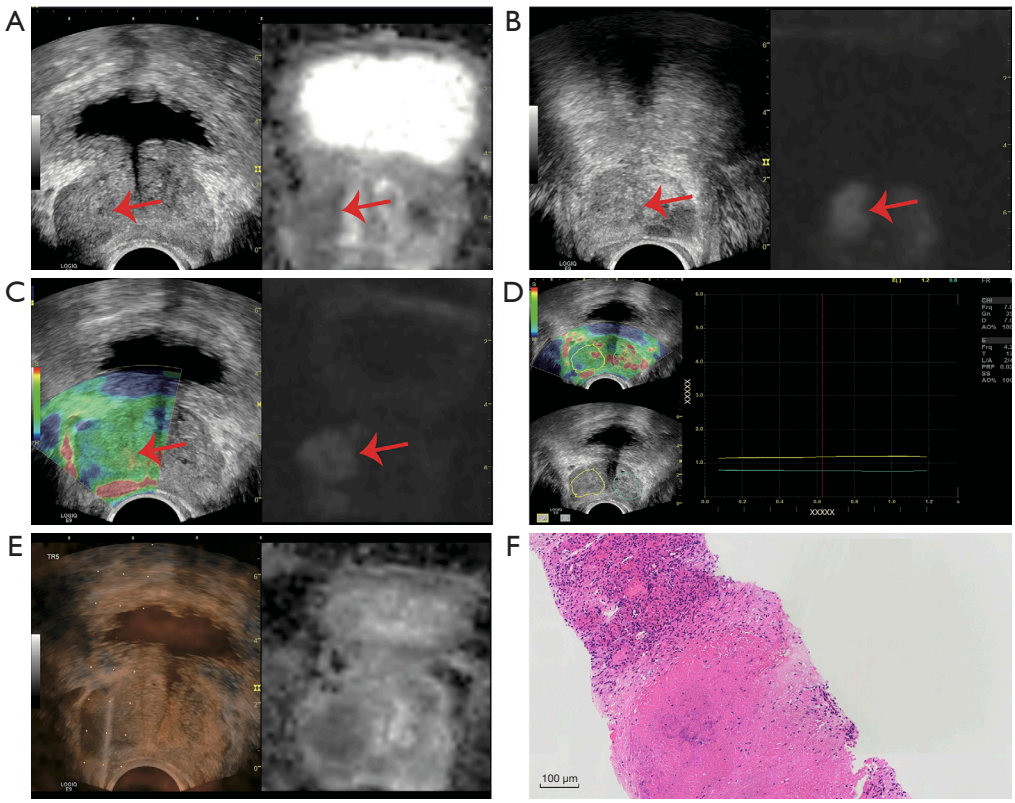

Figure 4 A 52-year-old patient with PSA =12.13 ng/mL, fPSA =1.15 ng/mL, and fPSA/PSA =0.095. (A) Pre-biopsy MRI revealed an abnormal signal area at the 7–11 o'clock position in the transition zone of the prostate, which was classified as PI-RADS 5. Elastography was performed in the imaging fusion state. (B) The image of the TRUS/MP-MRI fusion. (C) MRI revealed a suspicious area where was found by elastography that to be soft. (D) The EQS result of the suspicious zone was 1.1. (E) Targeted biopsy of the lesion, which was detected by MRI and elastography. (F) The targeted biopsy revealed prostatic tuberculosis (hematoxylin and eosin stain). Arrow: the target lesion. PSA, prostate-specific antigen; fPSA, free prostate-specific antigen; MRI, magnetic resonance imaging; PI-RADS, Prostate Imaging-Reporting and Data System; TRUS/MP-MRI, transrectal ultrasound/multi-parameter magnetic resonance imaging; EQS, elastographic Q-analysis score.

during 2,000 ms. It can avoid that selecting the single frame elastography you need for measurement. So EQS is more reliable than other instantaneous elastography.

Our study evaluated the PI-RADS score using the EQS and found that some PI-RADS 4–5 lesions were overestimated (36% all PI-RADS 4–5). Basing on statistical data, 70 prostate lesions (44.3% all PI-RADS 4–5) with the PI-RADS 4 or 5 were downgraded. Fifty-seven of them (81.4%) are benign nodules including one case of prostate tuberculosis. According to biopsy pathological results, we analysed the causes of this phenomenon.

In these 57 prostate lesions, more than half of the lesions showed infiltration of lymphocytes and other inflammatory cells. This often indicates the occurrence of prostatitis. Prostatitis is one of the common diseases of the prostate, and it is usually caused by *Escherichia coli* or *Staphylococcus* infection. As the condition worsens, it can eventually lead to the formation of an abscess (22). Both prostatitis and PCa can cause elevated PSA levels. At the same time, focal prostatitis or abscess could appear as a decreased signal on T2WI and increased perfusion on DCE-MRI. Depending on the PI-RADS version 2, the aforementioned findings could be scored at least 4/5, highly suggesting clinically significant PCa. However, on TRUS, it appears as a small honeycomb structure, with no obvious boundaries. During elastography, prostatitis is softer than PCa tissue (11). The elastogram shows that the lesion is usually green with a low EQS. A case of successful downgrade (*Figure 4*). When an abscess is formed, we can find a round region with inhomogeneous low signal on T2-WI, ring enhancement

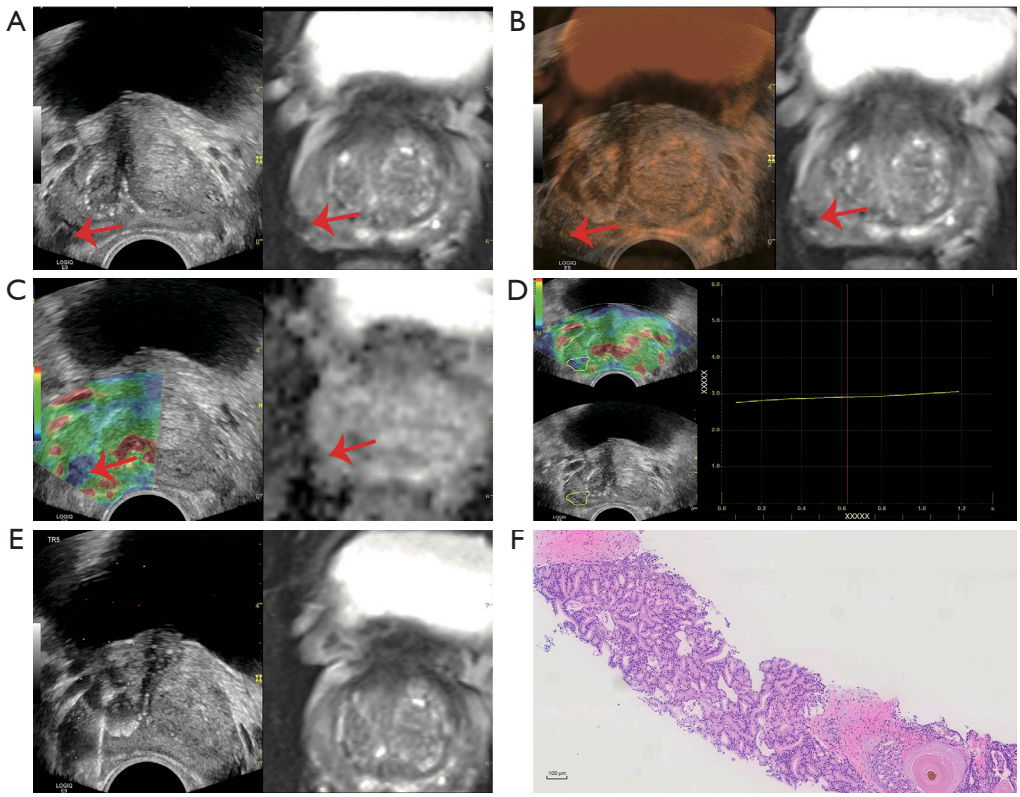

Figure 5 A 67-year-old patient with PSA =4.440 ng/mL, fPSA =0.560 ng/mL, and fPSA/PSA =0.126. (A) Pre-biopsy MRI revealed multiple lesions at the 8-o'clock position in the peripheral zone of the prostate, which was classified as PI-RADS 3. Elastography was performed in the imaging fusion state. (B) The overlay image of the TRUS/MP-MRI fusion. (C) Elastography revealed a suspicious area with increased local stiffness, which was detected by MRI. (D) The EQS result of the suspicious zone was 3.0. (E) Targeted biopsy of the lesion, which was detected by MRI and elastography. (F) The targeted biopsy revealed PCa (hematoxylin and eosin stain; Gleason score: 4+4 =8 and WHO/ISUP classification group: 4). Arrow: the target lesion. PSA, prostate-specific antigen; fPSA, free prostate-specific antigen; MRI, magnetic resonance imaging; PI-RADS, Prostate Imaging-Reporting and Data System; TRUS/MP-MRI, transrectal ultrasound/multi-parameter magnetic resonance imaging; EQS, elastographic Q-analysis score; PCa, prostate cancer; WHO/ISUP, World Health Organization/International Society of Urological Pathology.

on dynamic contrast-enhanced, and restriction on DWI. According to the PI-RADS version 2, this suggests clinically significant PCa, requiring biopsy. However, the elastographic appearances of the abscess are red and green, the same as with prostatitis, with a low EQS. There were 13 prostate lesions that we failed to downgrade to PI-RADS 3, eight of them were classified as Gleason score 3+3 or Gleason score 3+4, without clinical significance.

We also upgrade 36 prostate lesions with the PI-RADS 2 or 3 and EQS >1.85, but only six of them were PCa. A case of successful upgrade (*Figure 5*). Although upgrade-PI-RADS could improve the diagnosis of PCa, it generated more FP results. There are several reasons for this phenomenon. First, according to the ROC, specificity increases with the increase in the EQS. Second, the elastic ultrasound image quality is affected by the strength of the performer, especially those near the probe. When the strength is very high, false positivity is likely to occur. Third, lesions close to the inner urethra are prone to FP results, especially in those who have a catheter attachment. The balloon squeezes the inside of the urethra, making the surrounding tissues firmer. Despite this, the catheter can help us fuse the image better.

In this study, we confirmed that adding elastography into TRUS/MP-MRI fusion-guided biopsy could help improve the detection rate of PCa. Our previous research (23) was consistent with the conclusions of study by Brock *et al.* (21). The study by Ageeli *et al.* further confirmed the significant

correlation between elastography and Gleason score by radical prostatectomy (24). At the same, we expanded the sample size in this study, and analyzed the internal causes of this result from the pathological results.

From what has been discussed above, downgrade-PI-RADS was the best model because the high diagnostic sensitivity of MRI leads to too many FPs, and elastic ultrasound can just make up for this. If a prostate lesion's PI-RADS >3, and EQS ≤1.85, it is likely to be a benign lesion. If the prostate lesion's PI-RADS ≤3, and EQS >1.85, We should be cautious in diagnosing it as PCa, based on laboratory results and other relevant tests. Using this method to diagnose prostate disease could reduce the number of unnecessary biopsy procedures and prevent overdiagnosis. With the development of artificial intelligence (AI), it will integrate MRI with PI-RADS, elastography, and clinical laboratory data such as PSA, fPSA, e.g., to automate and rapidly obtain high-quality information to assist in clinical decision, like AI working in other areas of medical imaging (25).

There are several limitations to our study. Firstly, the quality of the elastography depends on the skill level of the physician, and thus, the examiner must be well trained. Secondly, the location of the lesion can affect the results. Lesions close to the inner urethra can easily lead to FP results. At last, all pathological results were based on biopsy specimens.

Conclusions

Using the EQS to supplement PI-RADS can improve the efficiency in diagnosing benign and malignant prostate lesions. The combination of the PI-RADS and the EQS with TRUS/MP-MRI fusion can not only improve the accuracy of PCa diagnosis but also reduce unnecessary biopsy procedures and prevent overdiagnosis. This technology compensates for the limitations of both ultrasound and MRI, particularly with downgrade-PI-RADS, could reduce FP results significantly in the differentiating between malignant and benign prostate lesions.

Acknowledgments

We would like to thank for the support and help of our D.team of Ultrasound Department Shenzhen People's Hospital.

Funding: This project was supported by the Commission of Science and Technology of Shenzhen (No. GJHZ20200731095401004).

Footnote

Reporting Checklist: The authors have completed the STARD reporting checklist. Available at https://qims.amegroups.com/article/view/10.21037/qims-21-932/rc

Conflicts of Interest: All authors have completed the ICMJE uniform disclosure form (available at https://qims.amegroups.com/article/view/10.21037/qims-21-932/coif). The authors have no conflicts of interest to declare.

Ethical Statement: The authors are accountable for all aspects of the work in ensuring that questions related to the accuracy or integrity of any part of the work are appropriately investigated and resolved. The study was conducted in accordance with the Declaration of Helsinki (as revised in 2013) and was approved by the Ethics Committee of our Shenzhen People's Hospital. All patients provided signed informed consent.

References

1. Siegel RL, Miller KD, Fuchs HE, Jemal A. Cancer Statistics, 2021. CA Cancer J Clin 2021;71:7-33.
2. Kumar V, Bora GS, Kumar R, Jagannathan NR. Multiparametric (mp) MRI of prostate cancer. Prog Nucl Magn Reson Spectrosc 2018;105:23-40.
3. Ahmed HU, El-Shater Bosaily A, Brown LC, Gabe R, Kaplan R, Parmar MK, Collaco-Moraes Y, Ward K, Hindley RG, Freeman A, Kirkham AP, Oldroyd R, Parker C, Emberton M; PROMIS study group. Diagnostic accuracy of multi-parametric MRI and TRUS biopsy in prostate cancer (PROMIS): a paired validating confirmatory study. Lancet 2017;389:815-22.
4. Frye TP, George AK, Kilchevsky A, Maruf M, Siddiqui

MM, Kongnyuy M, Muthigi A, Han H, Parnes HL, Merino M, Choyke PL, Turkbey B, Wood B, Pinto PA. Magnetic Resonance Imaging-Transrectal Ultrasound Guided Fusion Biopsy to Detect Progression in Patients with Existing Lesions on Active Surveillance for Low and Intermediate Risk Prostate Cancer. J Urol 2017;197:640-6.
5. Turkbey B, Rosenkrantz AB, Haider MA, Padhani AR, Villeirs G, Macura KJ, Tempany CM, Choyke PL, Cornud F, Margolis DJ, Thoeny HC, Verma S, Barentsz J, Weinreb JC. Prostate Imaging Reporting and Data System Version 2.1: 2019 Update of Prostate Imaging Reporting and Data System Version 2. Eur Urol 2019;76:340-51.
6. Panebianco V, Giganti F, Kitzing YX, Cornud F, Campa R, De Rubeis G, Ciardi A, Catalano C, Villeirs G. An update of pitfalls in prostate mpMRI: a practical approach through the lens of PI-RADS v. 2 guidelines. Insights Imaging 2018;9:87-101.
7. Ginat DT, Destounis SV, Barr RG, Castaneda B, Strang JG, Rubens DJ. US elastography of breast and prostate lesions. Radiographics 2009;29:2007-16.
8. Hwang SI, Lee HJ, Lee SE, Hong SK, Byun SS, Choe G. Elastographic Strain Index in the Evaluation of Focal Lesions Detected With Transrectal Sonography of the Prostate Gland. J Ultrasound Med 2016;35:899-904.
9. Brock M, von Bodman C, Palisaar RJ, Löppenberg B, Sommerer F, Deix T, Noldus J, Eggert T. The impact of real-time elastography guiding a systematic prostate biopsy to improve cancer detection rate: a prospective study of 353 patients. J Urol 2012;187:2039-43.
10. Tyloch DJ, Tyloch JF, Adamowicz J, Juszczak K, Ostrowski A, Warsiński P, Wilamowski J, Ludwikowska J, Drewa T. Elastography in prostate gland imaging and prostate cancer detection. Med Ultrason 2018;20:515-23.
11. Zhang Y, Tang J, Li YM, Fei X, Lv FQ, He EH, Li QY, Shi HY. Differentiation of prostate cancer from benign lesions using strain index of transrectal real-time tissue elastography. Eur J Radiol 2012;81:857-62.
12. Emara DM, Naguib NN, Yehia M, El Shafei MM. Ultrasound elastography in characterization of prostatic lesions: correlation with histopathological findings. Br J Radiol 2020;93:20200035.
13. Boehm K, Tennstedt P, Beyer B, Schiffmann J, Beckmann A, Michl U, Beyersdorff D, Budäus L, Graefen M, Karakiewicz PI, Salomon G. Additional elastography-targeted biopsy improves the agreement between biopsy Gleason grade and Gleason grade at radical prostatectomy. World J Urol 2016;34:805-10.
14. Ding Z, Jiao Y, Wu H, Zhang L, Song H, Ni Z, Ye X, Xu J, Dong F. Clinical Value of the Elastographic Q-Analysis Score in Assisting Real-Time Elastography-Guided Prostate Biopsy: A Retrospective Study of 125 Patients. J Ultrasound Med 2020;39:83-7.
15. Ding Z, Song D, Wu H, Tian H, Ye X, Liang W, Xu J, Dong F. Development and validation of a nomogram based on multiparametric magnetic resonance imaging and elastography-derived data for the stratification of patients with prostate cancer. Quant Imaging Med Surg 2021;11:3252-62.
16. Ding Z, Wu H, Song D, Tian H, Ye X, Liang W, Jiao Y, Hu J, Xu J, Dong F. Development and validation of a nomogram for predicting prostate cancer in men with prostate-specific antigen grey zone based on retrospective analysis of clinical and multi-parameter magnetic resonance imaging/transrectal ultrasound fusion-derived data. Transl Androl Urol 2020;9:2179-91.
17. Youden WJ. Index for rating diagnostic tests. Cancer 1950;3:32-5.
18. Kasivisvanathan V, Rannikko AS, Borghi M, et al. MRI-Targeted or Standard Biopsy for Prostate-Cancer Diagnosis. N Engl J Med 2018;378:1767-77.
19. Radtke JP, Wiesenfarth M, Kesch C, Freitag MT, Alt CD, Celik K, Distler F, Roth W, Wieczorek K, Stock C, Duensing S, Roethke MC, Teber D, Schlemmer HP, Hohenfellner M, Bonekamp D, Hadaschik BA. Combined Clinical Parameters and Multiparametric Magnetic Resonance Imaging for Advanced Risk Modeling of Prostate Cancer-Patient-tailored Risk Stratification Can Reduce Unnecessary Biopsies. Eur Urol 2017;72:888-96.
20. Ganzer R, Brandtner A, Wieland WF, Fritsche HM. Prospective blinded comparison of real-time sonoelastography targeted versus randomised biopsy of the prostate in the primary and re-biopsy setting. World J Urol 2012;30:219-23.
21. Brock M, Löppenberg B, Roghmann F, Pelzer A, Dickmann M, Becker W, Martin-Seidel P, Sommerer F, Schenk L, Palisaar RJ, Noldus J, von Bodman C. Impact of real-time elastography on magnetic resonance imaging/ultrasound fusion guided biopsy in patients with prior negative prostate biopsies. J Urol 2015;193:1191-7.
22. Porter CM, Shrestha E, Peiffer LB, Sfanos KS. The microbiome in prostate inflammation and prostate cancer. Prostate Cancer Prostatic Dis 2018;21:345-54.
23. Ding Z, Ye X, Zhang L, Sun Y, Ni Z, Liu H, Xu J, Dong F. Evaluation of the Performance of the Ultrasound (US) Elastographic Q-Analysis Score Combined With the Prostate Imaging Reporting and Data System for

Malignancy Risk Stratification in Prostate Nodules Based on Transrectal US-Magnetic Resonance Imaging Fusion Imaging. J Ultrasound Med 2019;38:2991-8.
24. Ageeli W, Wei C, Zhang X, Szewcyk-Bieda M, Wilson J, Li C, Nabi G. Quantitative ultrasound shear wave elastography (USWE)-measured tissue stiffness correlates with PIRADS scoring of MRI and Gleason score on whole-mount histopathology of prostate cancer: implications for ultrasound image-guided targeting approach. Insights Imaging 2021;12:96.
25. Greco F, Salgado R, Van Hecke W, Del Buono R, Parizel PM, Mallio CA. Epicardial and pericardial fat analysis on CT images and artificial intelligence: a literature review. Quant Imaging Med Surg 2022;12:2075-89.

Cite this article as: Tian H, Ding Z, Wu H, Yang K, Song D, Xu J, Dong F. Assessment of elastographic Q-analysis score combined with Prostate Imaging-Reporting and Data System (PI-RADS) based on transrectal ultrasound (TRUS)/multi-parameter magnetic resonance imaging (MP-MRI) fusion-guided biopsy in differentiating benign and malignant prostate. Quant Imaging Med Surg 2022;12(7):3569-3579. doi: 10.21037/qims-21-932

Supplementary

Table S1 New models distribution

Models	Total (n=318)	Benign (n=224)	Malignant (n=94)	P
Complex-PI-RADS, n [%]				<0.001
2	36 [11]	36 [16]	0 [0]	
3	157 [49]	141 [63]	16 [17]	
4	78 [25]	46 [21]	32 [34]	
5	47 [15]	1 [0]	46 [49]	
Upgrade-PI-RADS, n [%]				<0.001
2	36 [11]	36 [16]	0 [0]	
3	88 [28]	84 [38]	4 [4]	
4	141 [44]	101 [45]	40 [43]	
5	53 [17]	3 [1]	50 [53]	
Downgrade-PI-RADS, n [%]				<0.001
2	38 [12]	37 [17]	1 [1]	
3	192 [60]	170 [76]	22 [23]	
4	42 [13]	16 [7]	26 [28]	
5	46 [14]	1 [0]	45 [48]	

EQS, elastographic Q-analysis score; PSA, prostate-specific antigen; fPSA, free PSA; PSAD, PSA density; PI-RADS, prostate imaging-reporting and data system.

https://dx.doi.org/10.21037/qims-21-932